

The Gamma-ray Afterglows of Tidal Disruption Events

Xian Chen^{1*}, Germán Gómez-Vargas^{1,2,3} & James Guillochon^{4,5}

¹*Instituto de Astrofísica, Facultad de Física, Pontificia Universidad Católica de Chile, 782-0436 Santiago, Chile*

²*Instituto de Física, Pontificia Universidad Católica de Chile, Avenida Vicuña Mackenna 4860, Santiago, Chile*

³*Istituto Nazionale di Fisica Nucleare, Sezione di Roma “Tor Vergata”, I-00133 Roma, Italy*

⁴*Harvard-Smithsonian Center for Astrophysics, The Institute for Theory and Computation,
60 Garden Street, Cambridge, MA 02138, USA*

⁵*Einstein Fellow*

Draft 25 January 2019

ABSTRACT

A star wandering too close to a supermassive black hole (SMBH) will be tidally disrupted. Previous studies of such “tidal disruption event” (TDE) mostly focus on the stellar debris that are bound to the system, because they give rise to luminous flares. On the other hand, half of the stellar debris in principle are unbound and can steam to a great distance, but so far there is no clear evidence that this “unbound debris steam” (UDS) exists. Motivated by the fact that the circum-nuclear region around SMBHs is usually filled with dense molecular clouds (MCs), here we investigate the observational signatures resulting from the collision between an UDS and a MC, which is likely to happen hundreds of years after a TDE. We focus on γ -ray emission ($0.1 - 10^5$ GeV), which comes from the encounter of shock-accelerated cosmic rays with background protons and, more importantly, is not subject to extinction. We show that because of the high proton density inside the MC, the peak γ -ray luminosity is at least 100 times greater than that in the case without a MC (only with a smooth interstellar medium). The luminosity decays on a time-scale of decades, depending on the distance of the MC, and about a dozen of these “TDE afterglows” could be detected within a distance of about 16 Mpc by the future Cherenkov Telescope Array. Without careful discrimination, these sources potentially could contaminate the searches for starburst galaxies, galactic nuclei containing millisecond pulsars or dark-matter annihilation signals.

Key words: acceleration of particles — ISM: cosmic rays — galaxies: active — Local Group — gamma rays: galaxies

1 INTRODUCTION

A star wandering too close to a supermassive black hole (SMBH, with mass $M_\bullet \gtrsim 10^6 M_\odot$) would be tidally disrupted, an incident known as the “tidal disruption event” (TDE, Hills 1975; Rees 1988). The disruptive process starts when the tidal force exerted by the SMBH becomes comparable to the self-gravity of the star. Given the mass M_* and radius R_* of the star, this happens at a critical distance of $R_t \simeq R_*(M_\bullet/M_*)^{1/3}$ from the SMBH (Hills 1975). Since this “tidal radius” is tiny — it is merely $(M_\bullet/10^6 M_*)^{-2/3}$ times greater than the Schwarzschild radius of the SMBH — the TDE rate in a galaxy is usually low, about $\mathcal{O}(10^{-4})$ yr⁻¹ according to theoretical calculations (e.g. Magorrian & Tremaine 1999; Wang, Watarai & Mineshige 2004).

A fraction of the star after tidal disruption has a nega-

tive energy and remains gravitationally bound to the SMBH. Mutual collisions and the later accretion (by SMBH) of these bound stellar debris are expected to give rise to an electromagnetic outburst with a thermal spectrum, which peaks at UV and soft X-ray bands (Rees 1988). This “tidal flare” provides an effective means to reveal an otherwise dormant SMBH. So far tens of TDEs have been discovered in this way (see Komossa 2015, for a review).

In principle, about half of the debris released from the disrupted star would gain positive energies and escape from the system with a velocity asymptotically approaching $10^3 - 10^4$ km s⁻¹ (Rees 1988). Simulations showed that these unbound material would develop into an elongated “unbound debris stream” (UDS, Kochanek 1994; Guillochon et al. 2009, 2015; Coughlin & Nixon 2015). Two observational signatures directly associated with the UDS have been envisaged in the literature: (i) A brightening of Hydrogen lines several days after a TDE because of the recombination of the initially ionized plasma inside the UDS

* E-mail: xchen@astro.puc.cl

(Kasen & Ramirez-Ruiz 2010), and (ii) variability of optical emission lines on a time-scale of months to years due to the illumination of the UDS by the central tidal flare (Strubbe & Quataert 2009, 2011). While broad lines have been detected from TDEs (Gezari et al. 2012), the detected lines likely originate from the circularizing disk of debris (Guillochon, Manukian & Ramirez-Ruiz 2014) rather than the two aforementioned UDS signatures.

As a result, one important element in the current TDE model – that at least half of the stellar mass becomes unbound – remains untested. A possible cause of the non-detection is attenuation of optical/UV photons, by either the interstellar medium (ISM) close to SMBHs (Donley et al. 2002; Gezari et al. 2009) or a gaseous envelope shrouding the radiative material (Loeb & Ulmer 1997; Ulmer 1999; Strubbe & Quataert 2009; Metzger & Stone 2015; Miller et al. 2015). For this reason, it is important to look for signatures of UDSs in an electromagnetic waveband that is less subject to extinction, such as radio, infrared, hard X-ray or γ -ray bands.

Such a signature potentially could be generated by the collision of an UDS with the surrounding ISM. It has been realized since about two decades ago (Khokhlov & Melia 1996) that the UDS-ISM interaction will create a structure similar to a supernova remnant (SNR). Recently, we started investigating the radiation from this “unbound debris remnant” (UDR, Guillochon et al. 2015). We found that if it exists in an environment like the Galactic Centre (GC), the spectrum would peak in UV and soft X-ray, where extinction is still an issue. However, if a significant fraction of the collisional energy ends up in accelerating electrons, radio emission will be produced due to synchrotron radiation and the luminosity could amount to $\mathcal{O}(10^{37})$ erg s $^{-1}$ (assuming a TDE rate of 10^{-4} yr $^{-1}$). Given this luminosity, it is possible to detect $\mathcal{O}(1)$ such remnant in the GC, but not in other galaxies because the object would be too faint (Guillochon et al. 2015).

In our earlier studies of the UDR, we had not considered radiative mechanisms of hard photons, such as hard X-ray and γ -ray. It is worth mentioning that one way of generating hard X-rays/ γ -rays is by forming a jet, which can up-scatter low-energy photons to higher energies by inverse Compton process. This mechanism was introduced to explain the transient hard X-ray (15 – 50 keV) emission detected by *Swift* in three TDEs (Bloom et al. 2011; Burrows et al. 2011; Levan et al. 2011; Zauderer et al. 2011; Cenko et al. 2012; Brown et al. 2015). However, jets are not directly related to UDSs, therefore, jetted TDEs cannot be used for our purpose of looking for UDSs, not to mention the fact that the hard-X-ray/ γ -ray radiation from a jet is highly beamed so that the probability of seeing it is small.

Recently, an alternative way of producing γ -ray emission was proposed, originally to explain the possible excess of GeV γ -rays in the GC (Cheng, Chernyshov & Dogiel 2006, 2007; Cheng et al. 2011, 2012). This type of γ -ray emission is closely linked to the UDS-ISM collision. The collision basically generates a large amount of relativistic protons, known as cosmic rays (CRs), through a process called diffusive shock acceleration (Hinton & Hofmann 2009; Treumann 2009). The γ -ray emission is produced when the CRs escape from the shock region and start bombarding the non-relativistic protons in the ISM, leading to the formation of

neutral pions (π^0) which almost immediately decay into γ -rays ($\gtrsim 10$ MeV, Kafexhiu et al. 2014).

According to the calculations done for the GC (Cheng, Chernyshov & Dogiel 2006, 2007), the γ -ray luminosity would sustain at a level of about 10^{38} erg s $^{-1}$ if the TDE rate is 10^{-5} yr $^{-1}$. Given this luminosity, a γ -ray telescope whose sensitivity is typically 10^{-13} erg cm $^{-2}$ s $^{-1}$ at present (Funk, Hinton & CTA Consortium 2013) is able to detect the above source out to a distance of about 3 Mpc.

It is a good time to revisit this latter mechanism of γ -ray emission because of two instances of recent progress. (i) Excess of γ -ray (0.1 – 100 GeV) emission has been clearly detected in the GC (The Fermi-LAT Collaboration 2015), and possibly in two nearby dwarf galaxies (reported by Geringer-Sameth et al. 2015; Hooper & Linden 2015; Li et al. 2015, but see Drlica-Wagner et al. 2015 for a different result), by the Fermi Large Area Telescope (Fermi-LAT) on-board the Fermi Gamma-ray satellite. It is important to understand the contribution to these γ -ray emission by TDEs. (ii) Both theoretical and observational studies (see §2 for details) now suggest that around SMBHs the ISM is likely very clumpy, filled with long-lived molecular clouds (MCs). If UDSs collide with MCs, an enhancement of γ -ray emission is anticipated because the high proton density inside MC accelerates the production and the subsequent decay rate of CRs.

Motivated by the latest progress, we will analyze in this paper the γ -ray emission from the UDS-MC collision and investigate the prospect of detecting them in other galaxies. The paper is organized as follows. In §2 we briefly review the evidences supporting the ubiquity of MCs around SMBHs, and then we summarize the typical properties of such MCs. Then in §3 we describe the characteristics of a typical UDS, so that in §4 we can use them to evaluate the time-scales and the energetics related to the UDS-MC collision. Based on these results, we discuss in §5 the properties of the CRs produced by the collision. In §6 we calculate the luminosity and spectral energy distribution of the γ -ray emission resulting from the cooling of the above CRs inside the MCs of our interest. Using these results, we evaluate in §7 the number of point sources that can be detected by γ -ray telescopes. Three telescopes are considered here, namely, Fermi-LAT (Atwood et al. 2009), the High Energy Stereoscopic System (H.E.S.S., Aharonian et al. 2006) and the Cherenkov Telescope Array (CTA) currently under planning (Acharya et al. 2013). For completeness, in §8 we also calculate the γ -ray emission resulting from the interaction of UDSs with a smooth ISM, from which we infer the additional number of detectable sources. Finally, in §9 we discuss the possibility of detecting similar γ -ray sources in dwarf galaxies, due to the existence of intermediate massive black holes (IMBHs), and we also outline possible methods of separating our objects from other γ -ray sources.

2 MOLECULAR CLOUDS

There are at least three pieces of evidence suggesting that the ISM around SMBHs is very clumpy.

(i) It is now widely accepted that SMBHs grew mainly during the phase of active galactic nucleus (AGN). In the unified model of type-I/type-II AGNs, the most essential

ingredient is a torus-like structure of several parsecs in size composed of dusty gas clumps surrounding the central SMBH (Krolik & Begelman 1988; Antonucci 1993). Given the ubiquity of this structure in AGNs, it is natural to suspect that many SMBHs still have relic tori around them even though they are no longer active today.

(ii) Another evidence comes from a special type of galaxies only recently discovered (Komossa et al. 2008, 2009; Wang et al. 2012; Yang et al. 2013). These galaxies show peculiar iron and oxygen emission lines, which are atypical of a normal AGN but more consistent with a model in which an ionizing spectrum similar to that of a TDE is reflected by dense MCs (e.g. Wang et al. 2012). Besides, the line strength decays on a time-scale of several years, indicating that the reflectors reside within several parsecs from the central SMBHs (e.g. Komossa et al. 2008).

(iii) The most direct evidence is from the GC. Radio observations revealed tens of MCs at a distance of $0.5 - 2$ pc from Sgr A*, the SMBH in the GC (Mezger, Duschl & Zylka 1996). The densities of these MCs lie in a wide range of $n_H \sim (10^6 - 10^8) \text{ cm}^{-3}$ (Christopher et al. 2005), similar to what has been inferred for the MCs in those galaxies with peculiar line ratios (Wang et al. 2012). The spatial distribution and kinematics of the MCs in the GC are suggestive of a torus-like structure with a vertical thickness of about 0.5 pc at the inner edge (Christopher et al. 2005). Given these observed properties, the torus has a half-opening angle of about 27° and covers in total $f_c \sim 40\%$ of the sky when viewed from the central SMBH. It has been pointed out that such a geometry resembles that of a normal AGN torus (Mezger, Duschl & Zylka 1996; Ponti et al. 2013).

Based on these evidences, it seems likely that after a TDE, the UDS would collide with one of the MCs around the central SMBH. This collision differs in two ways from the interaction with a smooth ISM. (i) Because of the much higher proton density inside MC, the UDS loses its kinetic energy more rapidly (Guillochon et al. 2015), which implies a higher production rate of CRs. (ii) The CRs, after escaping from the shock region, are still inside a very dense environment (the MC), a condition favourable to π^0 formation. The second difference is also the main reason that those MCs close to supernova remnants (SNRs) often show an enhanced γ -ray emission (Aharonian & Atoyan 1996; Fatuzzo, Adams & Melia 2006; Gabici et al. 2015; H. E. S. S. Collaboration et al. 2015).

It is important to note that the MCs close to SMBHs are not the same as those seen in the Galactic plane. The former are orders of magnitude denser than the latter, and the reason is as follows. Given a typical distance of $D \sim 1$ pc between our MC and a SMBH, the Roche limit, which is a criterion for the MC to remain gravitationally bound, requires that

$$n_H \gtrsim M_\bullet / (m_p D^3) \simeq 4.1 \times 10^7 m_6 D_1^{-3} \text{ cm}^{-3}, \quad (1)$$

where m_p is the proton mass, $m_6 = M_\bullet / (10^6 M_\odot)$ and $D_1 = D / (1 \text{ pc})$. Therefore, when $D \sim 1 \text{ pc}$ and $M_\bullet \gtrsim 10^6 M_\odot$, we have $n_H \gtrsim 4 \times 10^7 \text{ cm}^{-3}$. This density is orders of magnitude higher than most MCs in the Galactic plane [$n_H \sim (10^2 - 10^3) \text{ cm}^{-3}$], and in fact even denser than the cores of normal MCs ($n_H \sim 10^5 \text{ cm}^{-3}$, Bodenheimer 2011).

Despite such a high density, the MCs around SMBHs do not collapse to form stars (Jeans instability), prob-

ably because they are not self-gravitating but confined mainly by an external agent, such as the surrounding hot and turbulent ISM, or the compressive tides of the central SMBHs (e.g. Chandrasekhar 1963; Shu 1992). In equilibrium with an external force, a MC could have a density significantly lower than what is required by the Roche limit (Chen, Amaro-Seoane & Cuadra 2015). For this reason, we chose $n_H = 10^7 \text{ cm}^{-3}$ as our fiducial value. This value agrees within a factor of $2 - 3$ with the mean density $4 \times 10^6 \text{ cm}^{-3}$ of those MCs in the GC, inferred from the brightness of molecular emission lines (optical-thin density from Christopher et al. 2005).

To complete our description of a MC, we take $R_c = 0.25$ pc as the fiducial radius, which is typical of the MCs in the GC as well (Christopher et al. 2005). Given this size and assuming that our MC is spherical and homogeneous, we can derive a mass of $M_c = 4\pi m_p n_H R_c^3 / 3 \sim 1.6 \times 10^4 n_7 M_\odot$ for the cloud, where $n_7 \equiv n_H / (10^7 \text{ cm}^{-3})$.

3 UNBOUND DEBRIS STREAMS

The evolution of an UDS in vacuum constitutes an important part of the initial conditions of our problem. Since a series of earlier works have studied this topic (Rees 1988; Kochanek 1994; Khokhlov & Melia 1996; Strubbe & Quataert 2009; Kasen & Ramirez-Ruiz 2010), we only summarize here the main results that are most relevant to our work, including the kinetic energy, internal velocity dispersion and the opening angle with respect to the central SMBH.

An UDS originates from the part of a star which at the time of tidal disruption has a positive energy. This unbound part contains about half of the mass of the star if the star initially approaches the SMBH along a parabolic orbit with a periapsis distance of R_t – an probable case in real galaxies (Rees 1988; Magorrian & Tremaine 1999). In this case, the unbound material distribute in a range of specific energy between $\mathcal{E} = 0$ and $\mathcal{E} = \mathcal{E}_0 = GM_\bullet R_* / R_t^2$ (Guillochon & Ramirez-Ruiz 2013; Stone, Sari & Loeb 2013). As a result, the total kinetic energy E_k of the UDS is

$$E_k = \int_0^{\mathcal{E}_0} \mathcal{E} \frac{dM}{d\mathcal{E}} d\mathcal{E} \simeq \frac{M_* \mathcal{E}_0}{4} \simeq 10^{50} \text{ erg } m_6^{1/3} m_*^{5/3} r_*^{-1}, \quad (2)$$

where $m_* \equiv M_*/M_\odot$, $r_* \equiv R_*/R_\odot$. Here we have assumed an even distribution of unbound material in specific energy, i.e. $dM/d\mathcal{E} = M_*/(2\mathcal{E}_0)$, which was proposed by Rees (1988) and later confirmed by smooth-particle hydrodynamics simulations (Evans & Kochanek 1989).

Although we made a couple simplifications to derive Equation (2), the result agrees well with the median value computed from a statistically representative ensemble of UDSs (Guillochon et al. 2015). Using this equation and the fact that $r_* \propto m_*^{0.6}$ for main-sequence stars at $m_* > 1$ (Demircan & Kahraman 1991; Gorda & Svechnikov 1998), we further derive $E_k \propto m_*^{1.1}$. This scaling relation indicates that more massive stars generally give rise to more energetic UDSs.

It is worth noting that Equation (2) does not include the additional gain of kinetic energy during the compression and bouncing of the star at the orbital periapsis

(Brassart & Luminet 2008, and references therein). We neglected it because the bouncing energy \mathcal{E}_b , about $\beta^2 GM_*/R_*$ per unit mass (Guillochon et al. 2009), is usually much smaller than \mathcal{E}_0 , where $\beta \equiv R_t/R_p$ is the so-called “penetration factor” defined as the ratio between R_t and the pericentre distance R_p of the initial stellar orbit.

Take tidal disruption of a solar-type star ($M_* = M_\odot$ and $R_* = R_\odot$) for example. When $M_\bullet = 4.3 \times 10^6 M_\odot$ which is the mass of the SMBH in the Milky Way (MW) (Genzel, Eisenhauer & Gillessen 2010), the penetration factor β cannot be greater than 4.3; otherwise the star will enter a radius smaller than the “innermost bound circular orbit” (twice the Schwarzschild radius for a non-rotating black hole) and eventually be swallowed as a whole by the SMBH. Given this limit to β , the ratio $\mathcal{E}_b/\mathcal{E}_0 \simeq \beta^2(M_*/M_\bullet)^{1/3}$ is small, in fact in the range (0.0063, 0.12).

We notice that our E_k differs by a factor of β^2 from that derived by Khokhlov & Melia (1996); Strubbe & Quataert (2009); Kasen & Ramirez-Ruiz (2010). This is because those authors calculated \mathcal{E}_0 using the formula $GM_\bullet R_*/R_p^2$, i.e. they assumed that the energy spread is determined at R_p instead of at R_t . However, recent studies of the tidal-disruption process suggest that using R_t is physically more appropriate (Guillochon & Ramirez-Ruiz 2013; Stone, Sari & Loeb 2013). Therefore, using R_p in the calculation will result in an overestimation of \mathcal{E}_0 by a factor of β^2 , which is non-negligible when $\beta > 1$.

Besides E_k , another important quantity of an UDS is its velocity. It determines the time of collision with a MC as well as the Mach number of the subsequent shock. It is important to realize that different parts of an UDS travel at different velocities because of the energy difference imprinted in different parts of the star at the time of tidal disruption. The fastest part has the highest specific energy, which, as we already know, is \mathcal{E}_0 . As a result, it has the highest velocity. When it has traveled to a distance of $D \gg R_t(M_\bullet/M_*)^{1/3}$, its velocity has asymptotically dropped to

$$v_0 \simeq \sqrt{2\mathcal{E}_0} \simeq 6.2 \times 10^3 \text{ km s}^{-1} m_6^{1/6} m_*^{1/3} r_*^{-1/2}. \quad (3)$$

Suppose the time $t = 0$ coincides with the time of stellar disruption, then the time at which the fastest part of the UDS has traversed a distance of D is

$$t_0 \simeq D/v_0 \simeq 1.6 \times 10^2 \text{ yr } m_6^{-1/6} m_*^{-1/3} r_*^{1/2} D_1. \quad (4)$$

For our interest $D \sim 1 \text{ pc} \gg R_t(M_\bullet/M_*)^{1/3}$. As for the part with a lower specific energy, i.e. $\mathcal{E} < \mathcal{E}_0$, it follows that the velocity asymptotically approaches $\sqrt{2\mathcal{E}}$ and it arrives at D later, around the time $t \simeq D/\sqrt{2\mathcal{E}}$.

Not only the velocities are different, the directions where different parts of an UDS are headed also differ (e.g. Kochanek 1994). In the equatorial plane – the plane defined by the initial orbit of the progenitor star – the difference is caused mainly by the energy spread \mathcal{E}_0 . The corresponding angular span relative to the central SMBH can amount to $2v_0/v_p$ when the self-gravity of UDS is negligible (Khokhlov & Melia 1996), where $v_p \simeq \sqrt{2GM_\bullet/R_p}$ is the mean stellar velocity during the pericentre passage. In the direction perpendicular to the equatorial plane, the angular span is caused by the bouncing velocity $v_\perp \simeq \beta\sqrt{GM_*/R_*}$ and is about $2v_\perp/v_p$ (Kasen & Ramirez-Ruiz 2010). From these angles, we derive a typical solid angle of $\Omega \simeq \pi v_0 v_\perp/v_p^2 = \pi [M_*/(2M_\bullet)]^{1/2}$ for UDSs.

According to the last formula, if a solar-type star is tidally disrupted by a SMBH with a mass of $M_\bullet = (10^6, 10^8) M_\odot$, we find that $\Omega = (2.2 \times 10^{-3}, 2.2 \times 10^{-4})$. These values are consistent with those from the earlier studies of UDSs, which showed that Ω generally lies in the range of $(10^{-4}, 10^{-2})$. It is known that the uncertainty is due partly to the different ways of calculating \mathcal{E}_0 (e.g. Khokhlov & Melia 1996; Strubbe & Quataert 2009; Kasen & Ramirez-Ruiz 2010 used R_p to calculate \mathcal{E}_0), and partly to the additional consideration of the effects of self-gravity (Kochanek 1994; Coughlin & Nixon 2015).

To account for these theoretical uncertainties, we parameterize Ω with $\Omega = 10^{-3}\Omega_{-3}$ and take $\Omega_{-3} = 1$ as our fiducial value. In any case, we find that Ω is much smaller than the typical solid angle, $\pi R_c^2/D^2 \simeq 0.20D_1^{-2}$, of those MCs considered in the previous section. This result indicates that an UDS interacts with only one MC at a time.

4 COLLISION BETWEEN UDS AND MC

So far we have specified the initial conditions of MCs and UDSs. Now we can proceed to study their collisions. Such a collision happens mostly likely at a distance of $\mathcal{O}(1) \text{ pc}$ from a SMBH, where MCs exist in large amount (§2). An UDS arriving at this distance is in a free-expansion phase, because the amount of ISM that has been swept up by the UDS is too small to affect the kinematics. For example, if the ISM surrounding the SMBH has a constant density of 10^4 cm^{-3} (as has been assumed by Khokhlov & Melia 1996; Cheng, Chernyshov & Dogiel 2006), the swept-up mass would be only $0.08D_1^3\Omega_{-3} M_\odot$. As a result, the UDS behaves in the same way as in vacuum until the time of collision, at about $t \simeq t_0$.

Immediately after the collision the UDS still continue its free expansion. But as it advances deeper into the dense MC, it soon sweeps up an amount of material that is as massive as the stream itself. When this happens, the free-expansion phase ends and a Sedov-like expansion follows. This phase transition occurs at a depth of

$$\Delta D \sim \frac{M_{\text{ej}}}{n_H m_p \Omega D^2} \simeq 0.0020 \text{ pc } m_* n_7^{-1} \Omega_{-3}^{-1} D_1^{-2} \quad (5)$$

from the surface of the MC, where $M_{\text{ej}} = 0.5M_*$ is the mass of the UDS. The fact that $\Delta D \ll R_c$ suggests that the MC is thick enough to stop the UDS completely. On the other hand, a normal MC like those in the Galactic plane cannot stop a UDS, because the density, typically of $10^2 - 10^3 \text{ cm}^{-3}$ (Bodenheimer 2011), would be too low.

Since the collisional velocity initially is about $v_s \sim v_0$, which is orders of magnitude higher than the typical (turbulent) sound speed $c_s \sim 20 \text{ km s}^{-1}$ in our MC (Genzel, Eisenhauer & Gillessen 2010), a strong shock will be produced. The shock efficiently dissipates the kinetic energy of the UDS, converting it into heat. To estimate the heating rate, we first recall that mass is injected into the collisional region at a rate of

$$\frac{dM}{dt} = \frac{dM}{d\mathcal{E}} \left| \frac{d\mathcal{E}}{dt} \right| \simeq \frac{M_*}{t_0} \left(\frac{t}{t_0} \right)^{-3}, \quad (6)$$

where $t \geq t_0$. The steep dependence on t implies that UDS

is head-heavy: From the arrival time of the fastest debris at $t = t_0$ to the time $1.4t_0$, already half of the mass of the UDS (50% of $M_*/2$) has been deposited into the MC, and in the following period of $0.6t_0$, much less matter (25% of $M_*/2$) arrives. Knowing the mass-injection rate dM/dt , we can calculate the energy-injection/heating rate with

$$\frac{dE_k}{dt} = \mathcal{E} \frac{dM}{dt} = \frac{4E_k}{t_0} \left(\frac{t}{t_0} \right)^{-5}. \quad (7)$$

The even steeper dependence on t indicates that kinetic energy is more concentrated at the head of the UDS than is mass: From $t = t_0$ to about $1.2t_0$, already 50% of the total kinetic energy has been injected, and by $t = 2t_0$ the injection of kinetic energy is about 94% complete.

To balance the heating rate, which is of order $E_k/t_0 \sim 2 \times 10^{40}$ ergs $^{-1}$ at the beginning of the collision, the surface temperature of the MC should rise to at least $T = 80$ K, so that the cooling rate $4\pi\sigma_S R_c^2 T^4$ (σ_S is the Stefan-Boltzmann constant) due to black-body radiation could be higher than 2×10^{40} ergs $^{-1}$. We note that most MCs detected in the GC do have a moderately high gas temperature, about 50 – 200 K (Genzel, Eisenhauer & Gillessen 2010), therefore, it seems that cooling would be effective.

Because of its ability of efficient cooling, our MC would not expand significantly even though the total energy injected by the UDS, E_k , greatly exceeds the gravitational binding energy of the cloud, which is about $E_c \sim GM_c^2/R_c \sim 2.4 \times 10^{49} n_7^2$ erg. On the other hand, in the (unlikely) case of insufficient cooling, the time-scale for our MC to expand is about $R_c/c_s \sim 2.4 \times 10^4$ yr, much longer than the collisional time-scale t_0 . Therefore, we can in any case neglect the dynamical evolution of the MC during the collision, which significantly simplifies our later analysis of the CR and γ -ray productions.

Before moving on to the next section, it is worth mentioning that the material immediately after the shock has an temperature of about $T_s \simeq 3m_p v_s^2/(16k_B)$ (Inoue et al. 2012; Pan, Patnaude & Loeb 2013, k_B is the Boltzmann constant), which is of order of 10^8 K for our system (also see Guillochon et al. 2015). Such a hot medium would emit X-rays, but it would be difficult to see directly this emission, because the MC of our interest has a column density of $n_H R_c \sim 6 \times 10^{24} n_7$ cm $^{-2}$, i.e. it is Compton thick. Consequently, the seed X-ray photons are likely absorbed inside the MC, and what can be seen are the reprocessed, low-energy photons (because $T \simeq 80$ K) emitted from the surface of the cloud.

5 COSMIC RAYS

It is well known that a strong shock like what we have just described in the previous section produces CRs. The mechanism, known as the diffusive shock acceleration, is well established due to the studies of SNRs (Hinton & Hofmann 2009). These earlier studies suggested that typically $\epsilon = 10\%$ of the kinetic energy injected into the shock region can be tapped to accelerate CRs, and those CRs escaping from the shock region follow a power-law distribution in the momentum space with an power-law index of $\gamma_0 \simeq 2$ (the “universal power law”, see review by Treumann 2009).

Applying these earlier results, we find that a total

amount of $\epsilon E_k \sim 10^{49}$ erg of CRs would be produced by the UDS-MC collision, and in the space of kinetic energy T_p , which is a more convenient frame for the later calculation of π^0 and γ -ray production, the CRs initially follow a spectrum of

$$dN_p/dT_p \propto (T_p + 1)/(T_p^2 + 2T_p)^{(\gamma_0+1)/2} \quad (8)$$

(also see Cheng, Chernyshov & Dogiel 2006, for the CR spectrum).

If $\gamma_0 \leq 2$, the CR spectrum must cut off at a maximum, $T_{p,\max}$, to avoid divergence of the total kinetic energy. This maximum energy in principle depends on the power of the shock, the duration of the particle-acceleration process and the strength of the magnetic field in the shock region. In practice, we will calculate $T_{p,\max}$ using the formula $10^2 v_3^2 t_2 B_{\text{mG}}$ TeV (Hinton & Hofmann 2009), where $v_3 = v_s/(10^3 \text{ km s}^{-1})$ characterizes the shock strength, $t_2 = t_s/(10^2 \text{ yr})$ is the shock-acceleration time-scale (t_s) in unit of 100 yr, and B_{mG} is the magnetic field strength in unit of mG. This formula is derived under the assumption of Bohm diffusion, which is the slowest diffusion process for particles to cross shock front. Correspondingly, it determines the lower limit of $T_{p,\max}$.

We now quantify the typical value of $T_{p,\max}$ in our model. Since the shock velocity initially is about v_0 and decays with time as $(t/t_0)^{-1}$ (§3), it follows that $v_s = (6000, 3800)$ km s $^{-1}$ when $t_s = t - t_0 = (10, 100)$ yr, where we have assumed $m_6 = m_* = r_* = D_1 = 1$. For B_{mG} , observations of the GC region showed that the magnetic field varies from 2 to 4 mG around the edge of the MCs (Yusef-Zadeh et al. 1996), and is about 0.2 mG in the field between those MCs (Crocker et al. 2005). Therefore, we assume $B_{\text{mG}} = 1$, and finally we find that $T_{p,\max} \simeq (0.36, 1.4)$ PeV when $(t - t_0) = (10, 100)$ yr. It is interesting to note that the $T_{p,\max}$ resulting from the interaction between UDSs and a smooth ISM also lies in the PeV range (Cheng et al. 2012). Therefore, UDSs are effective accelerators of PeV CRs.

The CRs escaping from the shock region will bombard the non-relativistic protons in the MC. A significant fraction of the subsequent proton-proton (pp) collisions are inelastic, so that the CRs gradually lose their kinetic energies and cool down. The pp -collision time-scale can be calculated with $(\sigma_{pp} n_{HC})^{-1}$, where $\sigma_{pp} \simeq 40$ mbarn is the total collisional cross section and c denotes the speed of light. Taking into account the inelasticity of the collision, usually parameterized by κ which has a value of about 0.45 (Fatuzzo, Adams & Melia 2006), we find a cooling time-scale of

$$\tau_{pp} = (\kappa \sigma_{pp} n_{HC})^{-1} \simeq 5.9 \text{ yr } n_7^{-1}. \quad (9)$$

During this period of τ_{pp} , a CR would have diffused in the MC by a length of $d \simeq (\mathcal{D} \tau_{pp})^{1/2}$, where \mathcal{D} is the diffusion coefficient. The typical value of \mathcal{D} for those MCs in the Galactic plane is about $\mathcal{D}(T_p) \simeq 10^{26} (T_p/10 \text{ GeV})^{1/2} \text{ cm}^2 \text{ s}^{-1}$ (Ormes, Ozel & Morris 1988; Torres, Marrero & de Cea Del Pozo 2010). However, for those in the GC, the value of \mathcal{D} is unclear except that it should be smaller because of the stronger magnetic field. For our purpose, we will use the diffusion coefficient of those normal MCs to derive an upper limit for d , and we find that

$$d \lesssim \sqrt{\mathcal{D}(T_p) \tau_{pp}} \simeq 0.25 \text{ pc } n_7^{-1/2} [T_p/(10 \text{ TeV})]^{1/4}. \quad (10)$$

Now it is clear that $d < R_c$ when $T_p < 10n_7^2$ TeV. These inequalities mean that a CR with a relatively low energy will be trapped inside MC because of cooling. In this case, the probability of π^0 production is the highest. On the other hand, when $T_p \gg 10n_7^2$ TeV, a CR may escape from the MC (depending on \mathcal{D} , which is still unconstrained). As a result, the kinetic energy of the CR is mostly lost, leading to a lower efficiency of π^0 production. We will consider this effect in the later calculation of the γ -ray spectrum resulting from π^0 decay.

So far we have neglected the energy loss of CRs due to collisional ionization. This type of energy loss is relatively unimportant because the corresponding time-scale, about $\tau_{\text{ion}} \sim 20 n_7^{-1} (T_p/1 \text{ GeV})$ years (Berezinskii et al. 1990), is longer than τ_{pp} , if we consider only the energy range relevant to π^0 production which is $T_p \gtrsim 0.3$ GeV.

6 GAMMA RAYS

6.1 Luminosity

Having characterized the CRs, we can now investigate the production of π^0 by pp collisions and calculate the subsequent γ -ray luminosity L_γ . We start from the formula (Fatuzzo, Adams & Melia 2006)

$$L_\gamma = \eta(\sigma_{pp} n_H c) E_{\text{CR}}(t), \quad (11)$$

where $E_{\text{CR}}(t)$ is the total energy of CRs inside a MC and $(\sigma_{pp} n_H c)$ is the collisional rate between a CR and the background protons. The factor η denotes the efficiency of π^0 production, and when γ_0 increases from 2 to 2.6, η decreases from 0.18 to 0.04 (Crocker et al. 2005).

In Equation (11) we deliberately wrote E_{CR} as a function of t , so as to draw attention to its time dependence, which we now elaborate. From the time $t = t_0$ when the UDS first hits the MC, to about $t_0 + \tau_{pp}$, the newly-produced CRs do not yet have time to cool down, so $E_{\text{CR}}(t)$ increases monotonically. For this reason, we derive $E_{\text{CR}}(t)$ by integrating $\epsilon dE_k/dt$, where $dE_k/dt \propto (t/t_0)^{-5}$ is the energy injection rate coming from Equation (7). The result is that $E_{\text{CR}}(t) = \epsilon E_k C(t)$, where the function $C(t) = 1 - (t/t_0)^{-4}$ comes from an integration of $(t/t_0)^{-5}$. Therefore, we know that the luminosity evolves as $L_\gamma = (\eta\epsilon/\kappa) E_k C(t)/\tau_{pp}$ when $t_0 < t < t_0 + \tau_{pp}$.

Afterwards ($t > t_0 + \tau_{pp}$) cooling becomes relevant. Consider now a time interval $(t, t + \tau_{pp})$ in this later stage. During this interval, the CRs produced earlier than t would have cool down completely and meanwhile a fresh amount of $\epsilon(dE_k/dt)\tau_{pp}$ of CRs would have been created. This consideration suggests that $E_{\text{CR}}(t) \sim \epsilon(dE_k/dt)\tau_{pp}$ at any moment of $t > t_0 + \tau_{pp}$. Now using Equation (11), we find that the corresponding luminosity is $L_\gamma \sim (\eta\epsilon/\kappa) dE_k/dt \propto (t/t_0)^{-5}$.

Figure 1 illustrates the evolution of L_γ as we have just described. We can see that (i) the γ -ray emission appears hundreds of years (depending on t_0) after the initial TDE, and (ii) the luminosity evolves on a time-scale of several decades (also depend on t_0). This behaviour is very different from that of a tidal flare, which already appears days after the moment of stellar disruption and lasts at most a couple of years (e.g. Rees 1988; Komossa 2015). To highlight this difference, in the following we will refer to the γ -ray signa-

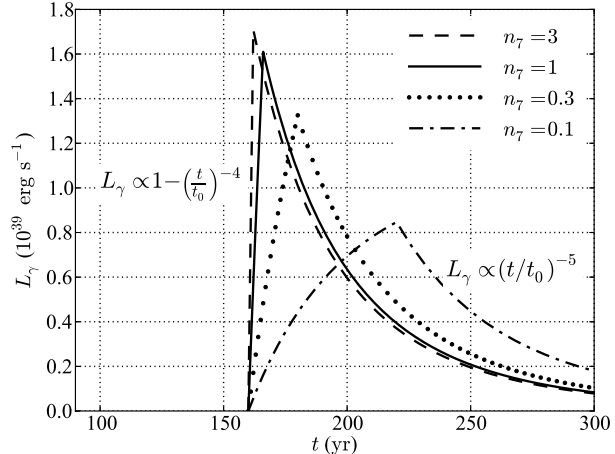


Figure 1. Light curves of the TDE afterglows, calculated using the following parameters, $(\epsilon_{-1}, \eta_{-1}, m_6, m_*, D_1) = (1, 1, 1, 1, 1)$. Different lines refer to MCs of different densities. In each calculation, the TDE happens at the time $t = 0$ and the UDS collides with the MC at the time $t_0 \simeq 160$ yr. Immediately after a collision, the γ -ray luminosity increases with time as $1 - (t/t_0)^{-4}$ because the newly-produced CRs do not have time to cool down and hence accumulate inside the MC. On a time-scale longer than τ_{pp} the luminosity drops as $(t/t_0)^{-5}$, because the injection of CRs is now relatively slow so that L_γ is limited by the energy-injection rate [Equation (7)].

ture resulting from the UDS-MC collision as the “afterglow” of TDE.

Figure 1 also shows that for a large range of n_H , the peak luminosity of the TDE afterglow is more or less constant, about 10^{39} erg s $^{-1}$. This result can be understood as a compromise between a higher π^0 production rate and a shorter CR cooling time when n_H increases. A more stringent proof of this insensitivity to n_H can be performed by evaluating L_γ at the moment $t = t_0 + \tau_{pp}$. Noticing that $\tau_{pp} \ll t_0$ when $n_H \gg 4 \times 10^5$ cm $^{-3}$, we can re-write $C(t_0 + \tau_{pp})$ as $4\tau_{pp}/t_0$, accurate to first-order, and consequently Equation (11) reduces to

$$L_{\text{peak}} = (\eta\epsilon/\kappa) 4E_k/t_0 \quad (12)$$

$$\simeq 1.6 \times 10^{39} \text{ erg s}^{-1} \epsilon_{-1} \eta_{-1} m_6^{1/2} m_*^{2} r_*^{-3/2} D_1^{-1}, \quad (13)$$

where we have normalized ϵ and η using their typical values such that $\epsilon_{-1} = \epsilon/0.1$ and $\eta_{-1} = \eta/0.1$. It is now clear that L_{peak} does not depend on n_H .

Although insensitive to n_H , L_{peak} does depend on other model parameters. To see more clearly the dependence, we adopt the relation $r_* \propto m_*^{0.6}$ for main-sequence stars with $m_* > 1$ (see references in §3) and derive $t_0 \propto m_6^{-1/6} m_*^{0.03} D_1$ and $L_\gamma \propto m_6^{1/2} m_*^{1.1} D_1^{-1}$. These scaling relations indicate that a closer MC, a more massive SMBH or tidal disruption of a more massive star generally leads to a brighter afterglow, but the time delay between an initial tidal flare and the later afterglow depends only on the location of the MC.

6.2 Spectrum

From an observational point of view, it is important to understand the spectral energy distribution of a γ -ray source,

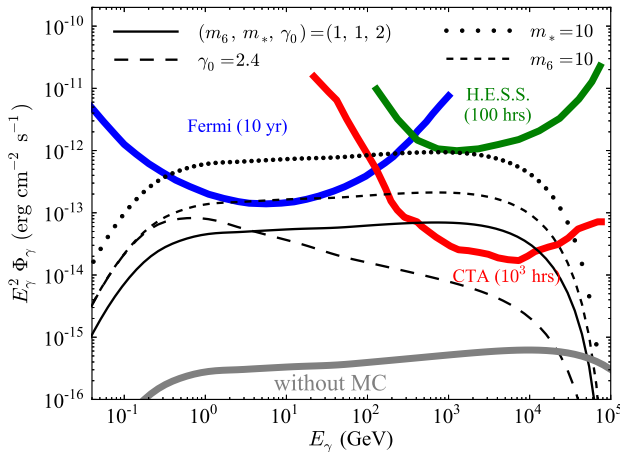


Figure 2. The γ -ray spectra of four representative TDE afterglows (thin black lines) located at the same distance of 5 Mpc. The model parameters, by default, are $(\epsilon_{-1}, m_6, m_*, D_1, \gamma_0) = (1, 1, 1, 1, 2)$ unless mentioned otherwise in the legend. For comparison, the thick grey line shows the typical γ -ray spectrum in the case without MCs, where an UDS interacts only with a smooth ISM of a density of $n_H = 10^4 \text{ cm}^{-3}$ (see §8 for details). The other three thick lines with blue, green and red colors are the sensitivity curves for, respectively, Fermi-LAT, H.E.S.S. and CTA.

because a γ -ray telescope is sensitive to only a limited energy band of photons.

To calculate the γ -ray spectrum of our TDE afterglow, we use the public code **LibppGam** (Kafexhiu et al. 2014). As an input to the code a CR spectrum is needed, and we use Equation (8) to compute it. We set the minimum energy of the CRs to 0.3 GeV, which is the γ -ray kinetic limit (Kafexhiu et al. 2014), and set the maximum energy to $T_{p,\text{max}} = 100 \text{ TeV}$, above which the CRs would escape from a MC of our interest (see §5). For illustrative purposes, we adopt $\epsilon E_k C(t_0 + \tau_{pp})$ as the total energy of CRs inside MC, where ϵ is fixed at our fiducial value 0.1. The corresponding total luminosity is equivalent to L_{peak} . It is worth mentioning that **LibppGam** calculates the CR-to-pion conversion efficiency based on particle physics, therefore, there is no need to specify η in the calculation.

Figure 2 shows four representative spectra (thin black curves) calculated in the above way. By default, the model parameters are $(\epsilon_{-1}, m_6, m_*, D_1, n_7, \gamma_0) = (1, 1, 1, 1, 1, 2)$ unless indicated otherwise. In these calculations, we have assumed a distance of 5 Mpc for the source. For comparison, the distance of the Andromeda Galaxy (M31) is about 0.8 Mpc, and the diameter of the Local Group is about 3 Mpc. A more thorough study of the effect of distance will be presented in the next section.

Figure 2 also shows that when $\gamma_0 = 2$ the γ -ray spectrum is relatively flat. This flatness reflects the fact that η is almost constant in a large range of energy band. This constancy also causes the steepening of the γ -ray spectrum when γ_0 increases to 2.4. In the following we will focus on the case $\gamma_0 = 2$ (the universal power law), motivated by the fact that the shock in our system has an extremely large Mach number (§4).

7 DETECTABILITY

To understand whether a TDE afterglow is detectable, we need first to know our instruments. Therefore, we consider here three γ -ray telescopes, namely, Fermi-LAT, H.E.S.S. and CTA, as representatives of the technology at present and in the near future.

We say that a telescope can “resolve” a TDE afterglow if part of the γ -ray spectrum is above the sensitivity curve of the telescope. This afterglow mostly likely will look like a point source if it is extragalactic given a typical angular resolution of 1 arcmin for a γ -ray telescope (e.g. see Funk, Hinton & CTA Consortium 2013, for CTA). Otherwise, if the entire spectrum is below the lowest point of the sensitivity curve, the object is “unresolvable”, and will only contribute to the diffuse extragalactic γ -ray background (Ackermann et al. 2015) in the field-of-view of the telescope.

The sensitivity curves of the three telescopes are shown in Figure 2. For H.E.S.S. and CTA, the sensitivity curves are adopted from Funk, Hinton & CTA Consortium (2013, 5σ detection), and for Fermi-LAT from its performance webpage¹. It is clear that CTA, due to its planned superior sensitivity, can resolve all the representative TDE afterglows except the one with $\gamma_0 = 2.4$; it is best suited to search for the TDE afterglows.

From now on, we will quantify the number N_γ of TDE afterglows resolvable by each of the three telescopes. At the end of this section, it will become clear that N_γ is small for Fermi-LAT and H.E.S.S., but is large enough for CTA to make a detection likely.

We will restrict the following analysis to a single population of TDE afterglows with the same SMBH masses (m_6), stars (m_*) and MCs (D_1). This simplification enables us to derive basic results that can be generalized in the future to account for multiple populations of afterglows. The generalization, however, requires knowledge that are currently unavailable, such as the space density of low-mass SMBHs ($M_\bullet \sim 10^6 M_\odot$, Stone & Metzger 2016) and the spatial distribution of MCs in other galaxies. For this reason, we have to postpone it to a future work. In this paper, we will circumvent these uncertainties by assigning a typical value to each of the parameters of (m_6, m_*, D_1) , according to the current understanding of TDEs and MCs.

Given the above restriction, we derive N_γ in three steps. (i) Estimate the maximum distance $r_\gamma(t)$ within which a source can be resolved by a given telescope. This maximum distance is a function of t (same definition as before and we consider only $t > t_0$) because the γ -ray luminosity decays with time as $L_\gamma(t) \simeq L_{\text{peak}}(t/t_0)^{-5}$. Since we are mostly interested in the case of $n_H > 10^6 \text{ cm}^{-3}$, we find that the rising phase (with a duration of τ_{pp}) before the luminosity peak is relatively short ($\tau_{pp} \ll t_0$ and also see Figure 1), so we have neglected its contribution to N_γ . (ii) Use $r_\gamma(t)$ to derive a detectable volume $V_\gamma(t) = 4\pi r_\gamma^3(t)/3$, and estimate the number $\Delta N_\gamma(t)$ of TDE afterglows that are inside this volume and are in the same time interval of $(t, t + \Delta t)$. (iii) Sum up the numbers $\Delta N_\gamma(t)$ in all intervals at $t > t_0$ to get N_γ .

We now address step (i). We know that $r_\gamma(t)$ is pro-

¹ http://www.slac.stanford.edu/exp/glast/groups/canda/lat_Performance.htm

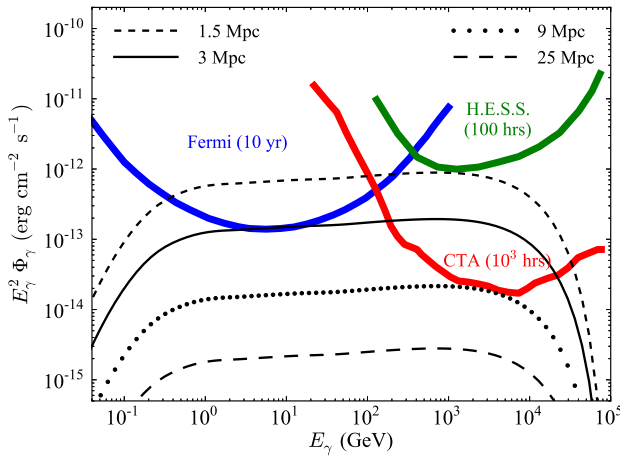


Figure 3. The spectra (thin black lines) of a TDE afterglow with $(\epsilon_{-1}, m_6, m_*, D_1, \gamma_0) = (1, 1, 1, 1, 2)$ at four different distances. The thick colored lines are the same telescope sensitivity curves as in Figure 2.

portional to $L_\gamma^{1/2}(t)$, and therefore to $L_{\text{peak}}^{1/2}(t/t_0)^{-5/2}$. Now substituting L_{peak} with Equation (13) and introducing a normalization factor r_0 that will be determined later, we derive

$$r_\gamma(t) \simeq r_0 \epsilon_{-1}^{1/2} m_6^{1/4} m_*^{0.55} D_1^{-1/2} (t/t_0)^{-5/2}. \quad (14)$$

We note that $r(t)$ does not depend on n_H because neither L_{peak} nor t_0 depends on it.

To quantify r_0 , we recall that $r_0 = r_\gamma(t_0)$ if we adopt the following parameters for our model $(\epsilon_{-1}, m_6, m_*, D_1) = (1, 1, 1, 1)$. Therefore, r_0 is the maximum distance within which a TDE afterglow with the above fiducial parameters can be resolved. We can find r_0 in Figure 3, which shows four spectra of the fiducial TDE afterglow at four different distances, assuming $t = t_0$ in the calculation. A comparison of these spectra with the sensitivity curves of the telescopes suggests that $r_0 \simeq 3, 1.5$ and 9 Mpc for Fermi-LAT, H.E.S.S. and CTA. Therefore, we find again that CTA is the most powerful among the instruments considered here to search for TDE afterglows.

In particular, using $r_0 = 9$ Mpc for CTA and the scaling relation $r_\gamma(t_0) \propto m_6^{1/4}$ presented in Equation (14), we find that $r_\gamma(t_0) \simeq 16$ Mpc if m_6 increases to 10, which is the most probable black-hole mass according to TDE observations (Stone & Metzger 2016). This detectable range already reaches the Virgo Cluster.

Knowing $r_\gamma(t)$, and therefore $V_\gamma(t)$, we can move on to step (ii). Since TDEs are a random process in time, we can calculate $\Delta N_\gamma(t)$ using the formula $\Delta N_\gamma(t) = f_c \Gamma V_\gamma(t) \Delta t$. The factor f_c denotes the fraction of the sky covered by MCs when viewed from a central SMBH. This covering factor determines the probability of an UDS to collide with a MC. In the following we adopt 40% as our fiducial value (see §1). The other parameter Γ is the volumetric TDE rate, an observable usually given in unit of $\text{Mpc}^{-3} \text{ yr}^{-1}$. Later in this section we will discuss the typical value of Γ .

In step (iii) we need to sum up all the $\Delta N_\gamma(t)$ for $t > t_0$. In the limit $\Delta t \ll t_0$, the summation is equivalent to the

integration $N_\gamma \simeq f_c \Gamma \int_{t_0}^{\infty} V_\gamma(t) dt$, which leads to

$$N_\gamma \simeq 12 \epsilon_{-1}^{3/2} m_*^{1.6} D_1^{-1/2} \Gamma_{-4} \left(\frac{f_c}{0.4} \right) \left(\frac{m_6}{10} \right)^{7/12} \left(\frac{r_0}{9 \text{ Mpc}} \right)^3, \quad (15)$$

where $\Gamma_{-4} \equiv \Gamma / (10^{-4} \text{ Mpc}^{-3} \text{ yr}^{-1})$. In Equation (15) we have normalized m_6 by 10 because, as has been mentioned before, it is the most typical value for the TDEs detected so far (Stone & Metzger 2016).

For Γ , a series of observational and theoretical studies have derived a wide range of values, between 10^{-7} and $10^{-4} \text{ Mpc}^{-3} \text{ yr}^{-1}$ (e.g. Magorrian & Tremaine 1999; Donley et al. 2002; Wang, Watarai & Mineshige 2004; Esquej et al. 2008; Gezari et al. 2009; van Velzen & Farrar 2014; Sun, Zhang & Li 2015; Holien et al. 2016; Stone & Metzger 2016). It is important to point out that these earlier works were studying TDEs at relatively large distances, in a redshift range of $0.01 \lesssim z \lesssim 1$ (Komossa 2015), so for their purposes the space density of SMBHs averages out to about $\mathcal{O}(10^{-2}) \text{ Mpc}^{-3}$ (e.g. Donley et al. 2002; Stone & Metzger 2016). We, however, are interested mainly in nearby SMBHs, because r_0 is relatively small. In the nearby universe there is apparently an overdensity of SMBHs – we already know three within a distance of 1 Mpc (the MW, M31 and M32, and see Kormendy & Ho 2013, for more SMBHs in the Local Group). To account for this overdensity, we will consider $\Gamma = 10^{-4} \text{ Mpc}^{-3} \text{ yr}^{-1}$ as our fiducial value, which corresponds to $\Gamma_{-4} = 1$.

Knowing the value of Γ , we now return to Equation (15). A CTA-like telescope corresponds to $r_0 = 9$ Mpc, so it could resolve about 12 TDE afterglows in all sky as point sources. This result also suggests that in order to detect $\mathcal{O}(10^2)$ TDE afterglows, a telescope four times more sensitive than CTA is needed. On the other hand, for Fermi-LAT N_γ would be about 27 times smaller, i.e. $N_\gamma < 0.5$, because $r_0 \simeq 3$ Mpc is three times smaller than before. The number N_γ for H.E.S.S. would be eight times even smaller because of the smaller r_0 .

Note that these numbers do not include the contributions from dwarf galaxies. Later §9 we will discuss the TDE afterglows in dwarf galaxies.

8 WITHOUT MCS

It is important to know what would happen if there were no MCs around SMBHs. In this case, neutral pions and γ -rays could still be generated by the interaction of UDSs with a smooth ISM. For the GC, earlier calculations showed that the corresponding γ -ray luminosity is as high as $10^{39} - 10^{40} \text{ erg s}^{-1}$ during the beginning of the interaction (Cheng, Chernyshov & Dogiel 2006, 2007; Cheng et al. 2011, 2012). Here we will revisit the calculation using the updated UDS model.

For the sake of comparison, we adopt the same ISM model as in the earlier studies – the ISM has a constant proton density of $n_H \sim 10^4 \text{ cm}^{-3}$ (Khokhlov & Melia 1996; Cheng, Chernyshov & Dogiel 2006). We will discuss the dependence of our results on n_H later in this section. Given this density, the characteristic length to stop UDS from free streaming, i.e. ΔD in Equation (5), increases to about $\Delta D' \simeq 2$ pc. Consequently, the Sedov-like expansion, dur-

ing which most CRs are produced, starts at about $t'_0 \simeq \Delta D'/v_0 \simeq 300$ yr.

Since t'_0 is much shorter than the proton cooling time-scale in the ISM, which is now about $\tau'_{pp} \simeq 5900$ yr according to Equation (9), we are allowed to treat the CR-injection process as an instantaneous event, and separate it from the later CR-cooling process. For this reason, we take $E'_{\text{CR}} = \epsilon E_k$ as the total energy of CRs eventually injected into the ISM.

Knowing n_H and E'_{CR} , we can calculate the γ -ray luminosity with

$$L'_\gamma = \eta(\sigma_{pp} n_H c) E_{\text{CR}} \quad (16)$$

$$\simeq 1.2 \times 10^{37} \text{ erg s}^{-1} \times \epsilon_{-1} \eta_{-1} m_6^{1/3} m_*^{1.1} n_4, \quad (17)$$

where $n_4 = n_H/(10^4 \text{ cm}^{-3})$. Unlike that in the case of UDS-MC interaction [Equation (13)], the luminosity here depends on the density n_H , because now it is limited not by the injection rate of CRs but the cooling rate. The evolution of the luminosity is also different: It rises on a time-scale of 300 years (t'_0) to reach L'_γ and then persists for about 6000 years (τ'_{pp}). To distinguish this γ -ray signature from the previous TDE afterglow, we call it the second-type afterglow.

As for the γ -ray spectrum, we calculate it following the same procedure described in §6.2, except for three modifications: (i) The total energy in CR is now E'_{CR} , (ii) the proton density in the background is set to 10^4 cm^{-3} and (iii) the maximum CR energy is $T_{p,\text{max}} = 1 \text{ PeV}$, adopted from Cheng et al. (2012). The result is shown in Figure 2 as the thick grey line. It clearly shows that without MCs, the γ -ray afterglow would be much fainter.

We note that the luminosity given by Equation (17) is more than 10^2 times smaller than the peak luminosity $10^{39} - 10^{40} \text{ erg s}^{-1}$ derived by Cheng, Chernyshov & Dogiel (2006, 2007), who considered a similar scenario of γ -ray emission following a TDE. This disparity is caused mainly by the much greater E'_{CR} used by Cheng et al. in their model, which is about $6 \times 10^{52} \text{ erg}$. Such a large energy is unlikely to be provided by an UDS (Guillochon et al. 2015), but a jet, whose formation may require special conditions not satisfied by most TDEs (De Colle et al. 2012).

Since the luminosity L'_γ is about 10^2 times lower than L_{peak} in §6.1, we expect the maximum distance at which a source is resolvable, r'_γ , to be 10 times smaller and the corresponding volume, V'_γ , to be 10^3 times smaller. These considerations lead to $r'_\gamma \simeq 0.9 \epsilon_{-1}^{1/2} \eta_{-1}^{1/2} m_6^{1/6} m_*^{0.55} n_4^{1/2} \text{ Mpc}$ for CTA. Correspondingly, the detectable volume is $V'_\gamma = 4\pi r'^3/3$. Now neither r'_γ nor V'_γ depend on time, because the γ -ray emission that we are considering now lasts from the time $t = t'_0$ to $t'_0 + \tau'_{pp}$ during which L'_γ is mostly constant.

Knowing the detection volume V'_γ and the duration τ'_{pp} of the second type of TDE afterglows, we can calculate the number of resolvable point sources N'_γ using the formula $\tau'_{pp} \Gamma V'_\gamma$. Note that the covering factor f_c does not appear here, because we assumed that the ISM distributes uniformly around a SMBH. With the parameters relevant to CTA, we derive that

$$N'_\gamma \simeq \tau'_{pp} \Gamma V'_\gamma \sim 6 \epsilon_{-1}^{3/2} \eta_{-1}^{3/2} m_*^{1.6} n_4^{1/2} \Gamma_{-4} \left(\frac{m_6}{10} \right)^{1/2}. \quad (18)$$

We expect these CTA sources to be relatively close to the earth, because $r'_\gamma \simeq 1.5(m_6/10)^{1/6} \text{ Mpc}$ when SMBHs with $m_6 = 10$ are considered. For the same reason given at the

end of §7, the number of point sources resolvable by Fermi-LAT and H.E.S.S. is extremely small.

In the above calculation, we have assumed $n_H = 10^4 \text{ cm}^{-3}$ for the sake of comparison. However, for the GC, theoretical models of the accretion flow onto the SMBH (Sgr A*) suggested that the ISM density gets as high as 10^4 cm^{-3} only within the central 10^{-3} pc (Yuan, Quataert & Narayan 2003). Moreover, observations of hot and X-ray-emitting ISM within a distance of 1 pc from Sgr A* showed that the ISM density is only $\mathcal{O}(10^2) \text{ cm}^{-3}$ on average (Baganoff et al. 2003). If the circum-nuclear media in other galaxies are similar to the ISM in the GC (Generozov, Stone & Metzger 2015), we would have a much lower value for n_H than what has been assumed above. Correspondingly, both L'_γ and N'_γ would be lowered, making it more difficult to detect the second type of TDE afterglows.

9 DISCUSSIONS

In this paper we have investigated a scenario likely to happen following a large number of TDEs (§1 and §2), in which the ejecta, or ‘‘UDS’’ (§3), launched from a disrupted star travels to a distance of $\mathcal{O}(1) \text{ pc}$ and collides into a MC. We have shown that the collision, which happens hundreds of years after the initial TDE, would produce a strong shock into the MC (§4), giving rise to a large amount of CRs with a kinetic energy as high as 1 PeV (§5). These CRs, after escaping from the shock region, would collide with the non-relativistic protons in the MC, producing π^0 and subsequently γ -rays in a wide energy range of $0.1 \sim 10^5 \text{ GeV}$ (§6). According to our calculation, this γ -ray signature, which we call ‘‘TDE afterglow’’, would be detectable by a CTA-like telescope out to a distance of $10-20 \text{ Mpc}$ (§7). On the other hand, if there were no MCs around SMBHs, there would be a second type of γ -ray afterglows resulting from the interaction of UDSs with a smooth ISM, which are much fainter than the first type (§8).

So far, we have not considered IMBHs ($10^3 \leq M_\bullet/M_\odot < 10^6$), which exist probably in the nuclei of many dwarf galaxies (Kormendy & Ho 2013). They produce TDE afterglows in the same way as SMBHs do, except that the luminosity is different. When an IMBH, $M_\bullet = 10^3 M_\odot$ for example, tidally disrupts a main-sequence star, the peak luminosity of the γ -ray afterglow would be $5 \times 10^{37} \text{ erg s}^{-1}$ according to Equation (13) (with MCs), or about $10^{36} n_4 \text{ erg s}^{-1}$ according to Equation (17) (without MCs). On the other hand, IMBHs are also able to tidally disrupt white dwarfs. If such an event happens, the kinetic energy of the UDS according to Equation (2) could significantly exceed 10^{50} erg , because a white dwarf is 10^2 times smaller than the sun. As a result, the γ -ray luminosity would be much higher.

Since dwarf galaxies have been found in large amount in the Local Universe, the number of TDE afterglows would also be large if IMBHs are ubiquitous. Intriguingly, Geringer-Sameth et al. (2015); Hooper & Linden (2015) recently reported a possible detection of γ -ray excess, about $5 \times 10^{33} \text{ erg s}^{-1}$ in the Fermi-LAT band, in a nearby dwarf galaxy Reticulum II (but see Drlica-Wagner et al. 2015, for a different result). This result immediately caused a debate about the origin of this γ -ray source, including dark-matter

annihilation (e.g. see [Diemand et al. 2008](#), for an earlier proposal). Our scenario of TDE afterglow can also explain the γ -ray luminosity of Reticulum II. For example, if a TDE with $M_\bullet = 10^3 M_\odot$ and $m_* = 1$ happened 3200 years ago, then after 500 years the UDS would have traversed a distance of 1 pc to hit a MC there (we find $t_0 \simeq 500D_1$ yr in this case), and today the γ -ray afterglow could have decayed to a luminosity of 5×10^{33} erg s $^{-1}$.

Since dark-matter annihilation, among with other sources such as star-bursts and a population of millisecond pulsars (MSPs), could also produce γ -rays above 1 GeV in galaxy centres ([Su, Slatyer & Finkbeiner 2010](#); [Abazajian et al. 2014](#); [Brandt & Kocsis 2015](#)), it is critical to find a way of separating these sources from our TDE afterglows.

We find that the γ -ray luminosities from dark-matter annihilation, probably about $\mathcal{O}(10^{37})$ erg s $^{-1}$ for a MW-like galaxy ([The Fermi-LAT Collaboration 2015](#)), and from MSPs, on average $10^{34} - 10^{35}$ erg s $^{-1}$ for one MSP ([Hooper & Mohlabeng 2015](#)), are both much lower than the peak luminosity of the first-type TDE afterglows, which, we now know, is about 10^{39} erg s $^{-1}$. This difference in luminosity could be used to distinguish TDE afterglows from the other two γ -ray sources. The limitation of this method is that it is effective for only “young” TDE afterglows. Because by the time of $t = (100)^{1/5}t_0 \simeq 2.5t_0$, the luminosity of the afterglow would have drop to 1% of its peak value, and it is no longer distinguishable from dark-matter-annihilation signal or a population of $\mathcal{O}(10^2)$ MSPs.

On the other hand, some star-burst galaxies could be as luminous as 10^{39} erg s $^{-1}$ ([The Fermi LAT Collaboration 2012](#)), and in this case a method other than comparing luminosities is needed. In the following we outline three methods that could be useful to separate the first type of TDE afterglows (UDS-MC-induced) from starburst galaxies.

(i) As we have seen in Figure 1, a TDE afterglow could be highly variable on a time-scale of ten years, especially at the beginning. On the other hand, the γ -ray emission from a star-burst (or a population of pulsars and dark-matter annihilation) is normally constant for (at least) million of years. Therefore, a variable γ -ray source with the characteristic luminosity $\mathcal{O}(10^{39})$ erg s $^{-1}$ and spectral index $\gamma_0 = 2$ would be a smoking-gun evidence for the first type of TDE afterglow.

(ii) In §5 we found that there is a critical kinetic energy, $T_p \sim 10n_7^2$ TeV, above which the CRs are able to escape from a MC before significantly losing their energies. Because of the existence of this critical energy, we expect a discontinuity visible in the γ -ray spectrum at a photon energy comparable to this critical energy – the intensity of the spectrum above this critical photon energy would be much lower than that below. Such a “spectral kink” lies in the sensitive window of CTA, and if detected, could provide another evidence for our first type of TDE afterglows. To better understand the time dependence, spectral shape and contrast of this discontinuity, it will be helpful to simulate the propagation of CRs inside a dense MC ($n_H \sim 10^7$ cm $^{-3}$).

(iii) The observations of star-formation galaxies by Fermi-LAT revealed a tight correlation between the γ -ray luminosity (L_γ in the band 0.1 – 100 GeV) and the luminosity in far-infrared (L_{FIR} , see [The Fermi LAT Collaboration](#)

[2012](#)). This correlation likely reflects a fundamental relationship between the star-formation rate (SFR) and the rate of CR production. According to this relationship, L_γ decreases linearly from about 10^{39} erg s $^{-1}$ when the SFR is about $1 M_\odot$ yr $^{-1}$ (like the MW), to about 10^{37} erg s $^{-1}$ where the SFR is about $10^{-2} M_\odot$ yr $^{-1}$ (such as the Small Magellanic Cloud). Correspondingly, L_{FIR} decreases from about 2×10^{43} erg s $^{-1}$ to 2×10^{41} erg s $^{-1}$. Based on these luminosities, it can be seen that if a TDE afterglow with $L_\gamma \sim 10^{39}$ erg s $^{-1}$ appears in a galaxy whose SFR is lower than $1 M_\odot$ yr $^{-1}$, L_γ in total would rise to above 10^{39} erg s $^{-1}$ but L_{FIR} is unaffected by the TDE afterglow, since the L_{FIR} of a TDE afterglow cannot exceed 10^{41} erg s $^{-1}$ according to the cooling rate calculated in §4. As a result, a galaxy hosting a TDE afterglow would appear as an outlier in the $L_\gamma - L_{\text{FIR}}$ diagram relative to the population of star-forming galaxies.

If CTA or more sensitive telescopes in the future do not detect any TDE afterglow, the non-detection, according to Equation (15), may be due to one or a combination of the following factors. (i) There is a deficiency of MCs in other galaxies so that f_c is much smaller than 0.4. (ii) MCs on average lie much further away from SMBHs than a distance of 1 pc. (iii) The volumetric TDE rate Γ in the local universe is much lower than 10^{-4} Mpc $^{-3}$ yr $^{-1}$. (iv) Or the current theory of the UDS from a TDE may be incomplete. These knowledges would help us better understand TDEs, as well as the stellar and gaseous environments around the SMBHs or IMBHs in normal galaxies.

ACKNOWLEDGMENTS

We thank Fukun Liu for pointing out the importance of tidal disruption of white dwarfs. XC is supported by CONICYT-Chile through Anillo (ACT1101). J. G. is supported by the NASA Einstein grant PF3-140108. GAGV is supported by Conicyt Anillo grant ACT1102, the Spanish MINECOs Consolider-Ingenio 2010 Programme under grant MultiDark CSD2009-00064 and also partly by MINECO under grant FPA2012-34694. Part of this work is carried out at the Astronomy Department of Peking University, supported by the “VRI concurso estadías en el extranjero” of PUC.

REFERENCES

- Abazajian K. N., Canac N., Horiuchi S., Kaplinghat M., 2014, *Phys. Rev. D*, 90, 023526
- Acharya B. S. et al., 2013, *Astroparticle Physics*, 43, 3
- Ackermann M., Ajello M., Albert A., et al., 2015, *ApJ*, 799, 86
- Aharonian F. et al., 2006, *A&A*, 457, 899
- Aharonian F. A., Atoyan A. M., 1996, *A&A*, 309, 917
- Antonucci R., 1993, *ARA&A*, 31, 473
- Atwood W. B. et al., 2009, *ApJ*, 697, 1071
- Baganoff F. K. et al., 2003, *ApJ*, 591, 891
- Berezinskii V. S., Bulanov S. V., Dogiel V. A., Ptuskin V. S., 1990, *Astrophysics of cosmic rays*
- Bloom J. S., Giannios D., Metzger B. D., et al., 2011, *Science*, 333, 203
- Bodenheimer P. H., 2011, *Principles of Star Formation*

Brandt T. D., Kocsis B., 2015, *ApJ*, 812, 15

Brassart M., Luminet J.-P., 2008, *A&A*, 481, 259

Brown G. C., Levan A. J., Stanway E. R., Tanvir N. R., Cenko S. B., Berger E., Chornock R., Cucchiaria A., 2015, *MNRAS*, 452, 4297

Burrows D. N., Kennea J. A., Ghisellini G., et al., 2011, *Nature*, 476, 421

Cenko S. B., Krimm H. A., Horesh A., et al., 2012, *ApJ*, 753, 77

Chandrasekhar S., 1963, *ApJ*, 138, 1182

Chen X., Amaro-Seoane P., Cuadra J., 2015, arXiv:1506.08196

Cheng K. S., Chernyshov D. O., Dogiel V. A., 2006, *apj*, 645, 1138

Cheng K. S., Chernyshov D. O., Dogiel V. A., 2007, *A&A*, 473, 351

Cheng K.-S., Chernyshov D. O., Dogiel V. A., Ko C.-M., Ip W.-H., 2011, *ApJ*, 731, L17

Cheng K.-S., Chernyshov D. O., Dogiel V. A., Ko C.-M., Ip W.-H., Wang Y., 2012, *ApJ*, 746, 116

Christopher M. H., Scoville N. Z., Stolovy S. R., Yun M. S., 2005, *ApJ*, 622, 346

Coughlin E. R., Nixon C., 2015, *ApJ*, 808, L11

Crocker R. M., Fatuzzo M., Jokipii J. R., Melia F., Volkas R. R., 2005, *ApJ*, 622, 892

De Colle F., Guillochon J., Naiman J., Ramirez-Ruiz E., 2012, *ApJ*, 760, 103

Demircan O., Kahraman G., 1991, *Ap&SS*, 181, 313

Diemand J., Kuhlen M., Madau P., Zemp M., Moore B., Potter D., Stadel J., 2008, *Nature*, 454, 735

Donley J. L., Brandt W. N., Eracleous M., Boller T., 2002, *AJ*, 124, 1308

Drlica-Wagner A., Albert A., Bechtol K., et al., The DES Collaboration, 2015, *ApJ*, 809, L4

Esquej P. et al., 2008, *A&A*, 489, 543

Evans C. R., Kochanek C. S., 1989, *ApJ*, 346, L13

Fatuzzo M., Adams F. C., Melia F., 2006, *ApJ*, 653, L49

Funk S., Hinton J. A., CTA Consortium, 2013, *Astroparticle Physics*, 43, 348

Gabici S., Krause J., Morlino G., Nava L., 2015, in *European Physical Journal Web of Conferences*, Vol. 105, *European Physical Journal Web of Conferences*, p. 2001

Generozov A., Stone N. C., Metzger B. D., 2015, *MNRAS*, 453, 775

Genzel R., Eisenhauer F., Gillessen S., 2010, *Reviews of Modern Physics*, 82, 3121

Geringer-Sameth A., Walker M. G., Koushiappas S. M., Koposov S. E., Belokurov V., Torrealba G., Evans N. W., 2015, *Physical Review Letters*, 115, 081101

Gezari S. et al., 2012, *Nature*, 485, 217

Gezari S. et al., 2009, *ApJ*, 698, 1367

Gorda S. Y., Svechnikov M. A., 1998, *Astron. Rep.*, 42, 793

Guillochon J., Manukian H., Ramirez-Ruiz E., 2014, *ApJ*, 783, 23

Guillochon J., McCourt M., Chen X., Johnson M. D., Berger E., 2015, arXiv:1509.08916

Guillochon J., Ramirez-Ruiz E., 2013, *ApJ*, 767, 25

Guillochon J., Ramirez-Ruiz E., Rosswog S., Kasen D., 2009, *ApJ*, 705, 844

H. E. S. S. Collaboration et al., 2015, *A&A*, 574, A100

Hills J. G., 1975, *Nature*, 254, 295

Hinton J. A., Hofmann W., 2009, *ARA&A*, 47, 523

Holoi T. W.-S., Kochanek C. S., Prieto J. L., et al., 2016, *MNRAS*, 455, 2918

Hooper D., Linden T., 2015, *JCAP*, 9, 16

Hooper D., Mohlabeng G., 2015, arXiv:1512.04966

Inoue T., Yamazaki R., Inutsuka S.-i., Fukui Y., 2012, *ApJ*, 744, 71

Kafexhiu E., Aharonian F., Taylor A. M., Vila G. S., 2014, *Phys. Rev. D*, 90, 123014

Kasen D., Ramirez-Ruiz E., 2010, *ApJ*, 714, 155

Khokhlov A., Melia F., 1996, *ApJ*, 457, L61

Kochanek C. S., 1994, *ApJ*, 422, 508

Komossa S., 2015, *Journal of High Energy Astrophysics*, 7, 148

Komossa S. et al., 2009, *ApJ*, 701, 105

Komossa S. et al., 2008, *ApJ*, 678, L13

Kormendy J., Ho L. C., 2013, *ARA&A*, 51, 511

Krolik J. H., Begelman M. C., 1988, *ApJ*, 329, 702

Levan A. J., Tanvir N. R., Cenko S. B., et al., 2011, *Science*, 333, 199

Li S. et al., 2015, arXiv:1511.09252

Loeb A., Ulmer A., 1997, *ApJ*, 489, 573

Magorrian J., Tremaine S., 1999, *MNRAS*, 309, 447

Metzger B. D., Stone N. C., 2015, arXiv:1506.03453

Mezger P. G., Duschl W. J., Zylka R., 1996, *A&ARv*, 7, 289

Miller J. M. et al., 2015, *Nature*, 526, 542

Ormes J. F., Ozel M. E., Morris D. J., 1988, *ApJ*, 334, 722

Pan T., Patnaude D., Loeb A., 2013, *MNRAS*, 433, 838

Ponti G., Morris M. R., Terrier R., Goldwurm A., 2013, in *Advances in Solid State Physics*, Vol. 34, *Cosmic Rays in Star-Forming Environments*, Torres D. F., Reimer O., eds., p. 331

Rees M. J., 1988, *Nature*, 333, 523

Shu F. H., 1992, *The physics of astrophysics. Volume II: Gas dynamics*.

Stone N., Sari R., Loeb A., 2013, *MNRAS*, 435, 1809

Stone N. C., Metzger B. D., 2016, *MNRAS*, 455, 859

Strubbe L. E., Quataert E., 2009, *MNRAS*, 400, 2070

Strubbe L. E., Quataert E., 2011, *MNRAS*, 415, 168

Su M., Slatyer T. R., Finkbeiner D. P., 2010, *ApJ*, 724, 1044

Sun H., Zhang B., Li Z., 2015, *ApJ*, 812, 33

The Fermi LAT Collaboration, 2012, *ApJ*, 755, 164

The Fermi-LAT Collaboration, 2015, arXiv:1511.02938

Torres D. F., Marrero A. Y. R., de Cea Del Pozo E., 2010, *MNRAS*, 408, 1257

Treumann R. A., 2009, *A&ARv*, 17, 409

Ulmer A., 1999, *ApJ*, 514, 180

van Velzen S., Farrar G. R., 2014, *ApJ*, 792, 53

Wang J.-M., Watarai K.-Y., Mineshige S., 2004, *ApJ*, 607, L107

Wang T.-G., Zhou H.-Y., Komossa S., Wang H.-Y., Yuan W., Yang C., 2012, *ApJ*, 749, 115

Yang C.-W., Wang T.-G., Ferland G., Yuan W., Zhou H.-Y., Jiang P., 2013, *ApJ*, 774, 46

Yuan F., Quataert E., Narayan R., 2003, *ApJ*, 598, 301

Yusef-Zadeh F., Roberts D. A., Goss W. M., Frail D. A., Green A. J., 1996, *ApJ*, 466, L25

Zauderer B. A., Berger E., Soderberg A. M., et al., 2011, *Nature*, 476, 425